CHIN. PHYS. LETT. Vol. 38, No. 9 (2021) 094202 **Express Letter**

Synchronization and Phase Shaping of Single Photons with High-Efficiency Quantum Memory

Keyu Su(苏柯宇)[1†], Yunfei Wang(王云飞)[1†*], Shanchao Zhang(张善超)[1,2†], Zhuoping Kong(孔焯平)[1], Yi Zhong(钟艺)[1], Jianfeng Li(李建锋)[1], Hui Yan(颜辉)[1,2,3*], and Shi-Liang Zhu(朱诗亮)[1,2*]

[1]*Guangdong Provincial Key Laboratory of Quantum Engineering and Quantum Materials, School of Physics and Telecommunication Engineering, South China Normal University, Guangzhou 510006, China*
[2]*Guangdong-Hong Kong Joint Laboratory of Quantum Matter, Frontier Research Institute for Physics, South China Normal University, Guangzhou 510006, China*
[3]*Guangdong Provincial Engineering Technology Research Center for Quantum Precision Measurement, South China Normal University, Guangzhou 510006, China*

(Received 22 July 2021; accepted 15 August 2021; published online 2 September 2021)

Time synchronization and phase shaping of single photons both play fundamental roles in quantum information applications that rely on multi-photon quantum interference. Phase shaping typically requires separate modulators with extra insertion losses. Here, we develop an all-optical built-in phase modulator for single photons using a quantum memory. The fast phase modulation of a single photon in both step and linear manner are verified by observing the efficient quantum-memory-assisted Hong–Ou–Mandel interference between two single photons, where the anti-coalescence effect of bosonic photon pairs is demonstrated. The developed phase modulator may push forward the practical quantum information applications.

DOI: 10.1088/0256-307X/38/9/094202

Multi-photon interference of quantum light, like single photons, lies at the heart of quantum information applications such as realizing quantum computing with linear optics and building large-scale quantum networks,[1−6] which demands both the phase control and the timing synchronization operation of those photons. On the one hand, phase degrees of those single photons not only play a fundamental role in manipulating the interference but also can be utilized to encode quantum information in quantum information applications protocols.[7−10] Hence, efficiently manipulating the phase of single photons is always desired for multi-photon interference. Separate optical elements, e.g., electro-optic phase modulator, are usually used to shape a single photon's phase,[11] which may inevitably reduce the multi-photon interference rate in the practical applications.[7] On the other hand, quantum memories (QMs) that can store and readout single photons on-demand has been explored and demonstrated to be necessary for multi-photon interferometer[12−14] and large-scale quantum information applications.[7,15−18] Therefore, developing a single device that can both synchronize single photons and simultaneously control their phases would push forward the practical quantum information applications.

QMs have been built based on various coherent quantum processes, such as electromagnetically induced transparency (EIT)[19−22] and Raman schemes.[23−25] The intrinsic coherence offers a promising way to tune the phase of light in the write and readout procedure,[26−30] which have also been implied by various experiments using weak laser pulses.[31−33] However, up to now, there have been no direct demonstration of phase control of quantum light such as a single photon using these schemes.

In this work, using an efficient EIT-based QM, we firstly show a QM-assisted Hong–Ou–Mandel (HOM) interference by synchronizing the single photons spontaneously generated from two cold atomic ensembles, where the detectable interference event rate is improved by a factor of 15 compared to the case without a QM. By phase-modulating the control laser of the QM, we demonstrate an all-optical phase modulation of single photons while keeping the high storage efficiency of 86%. Controllable coalescence and anti-coalescence behaviors of single photons are observed when the phase of readout single photons are phase

Supported by the National Key Research and Development Program of China (Grant No. 2020YFA0309500), the Key-Area Research and Development Program of Guangdong Province (Grant No. 2019B030330001), the Key Project of Science and Technology of Guangzhou (Grant No. 2019050001), and the National Natural Science Foundation of China (Grant Nos. 11822403, 62005082, 12004120, U20A2074, and U1801661), the Natural Science Foundation of Guangdong Province (Grant No. 2018A0303130066), the China Postdoctoral Science Foundation (Grant No. 2020M672681), and the Guangdong Basic and Applied Basic Research Foundation (Grant No. 2020A1515110848).
†These authors contributed equally to this work.
*Corresponding authors. Email: yunfeiwang2014@126.com; yanhui@scnu.edu.cn; slzhu@scnu.edu.cn
© 2021 Chinese Physical Society and IOP Publishing Ltd

modulated in both step and linear way. Our work verifies that both the coherence and quantum nature of single photons can be preserved well when modulated by a QM built-in phase modulator and may have promising applications in practical quantum information processing.

The storage and readout procedure of a single photon in an EIT-base quantum memory (QM) can be well described by the dynamics of dark-state polariton[26] inside an atomic ensemble including homogeneously distributed N atoms:

$$\hat{\Psi}(z,t) = \cos\theta(t)\hat{\psi}(z,t) - \sin\theta(t)\sqrt{N}\hat{S}(z,t), \quad (1)$$

where $\hat{\psi}(z,t)$ refers to the spatial-temporal envelope of photon field inside the atomic ensemble and $\hat{S}(z,t)$ is the envelope of atomic spin wave; $\tan\theta(t) = \frac{g\sqrt{N}}{\Omega_c(t)}$ with $\Omega_c(t)$ as the Rabi frequency of control laser and g as the atom-photon coupling constant. Considering a typical storage procedure with initial constant $\Omega_c(t<0) = \Omega_w$, a single photon entering the atomic ensemble from the vacuum ($N = 0$) would excite an atomic spin wave $\hat{S}(z,t) = \frac{g}{\Omega_w}\hat{\psi}(z,t)$. Then, the control laser is adiabatically switched off and kept off during $0 \le t \le t_r$ to store the envelope profile of photon field into the stationary spin wave $\hat{S}(z,t) = \hat{S}(z,0)$ with zero group velocity $v_g = c_0 * \cos\theta(t) = 0$ with c_0 as the light speed in vacuum [see Eq. (11) in Ref. [26]].

When readout procedure starts, a control laser is switched on at $t = t_r$ with envelope of $\Omega_r(t - t_r)e^{-i\phi_r(t-t_r)}$. The propagating dark-state polariton $\hat{\Psi}(z,t)$ are adiabatically re-built up with $\hat{S}(z, t \ge t_r) = \frac{g\hat{\psi}_r(z,t-t_r)}{\Omega_r(t-t_r)e^{-i\phi_r(t-t_r)}}$, which eventually leave the atomic ensemble and is transformed into a readout photon field in vacuum. In the above ideal storage-readout process, the input and readout photon field are connected by $\hat{S}(z,t_r) = \hat{S}(z,0)$ with the following relation, except a global undetermined dynamical phase factor $e^{-i\phi_{s0}}$ that might be acquired in experiment due to control laser phase fluctuation, atomic spin wave dynamics and so on:

$$\hat{\psi}_r(z, t - t_r) = \hat{\psi}(z,t)\frac{\Omega_r(t_r)e^{-i\phi_r(t_r)}}{\Omega_w e^{i\phi_{s0}}}. \quad (2)$$

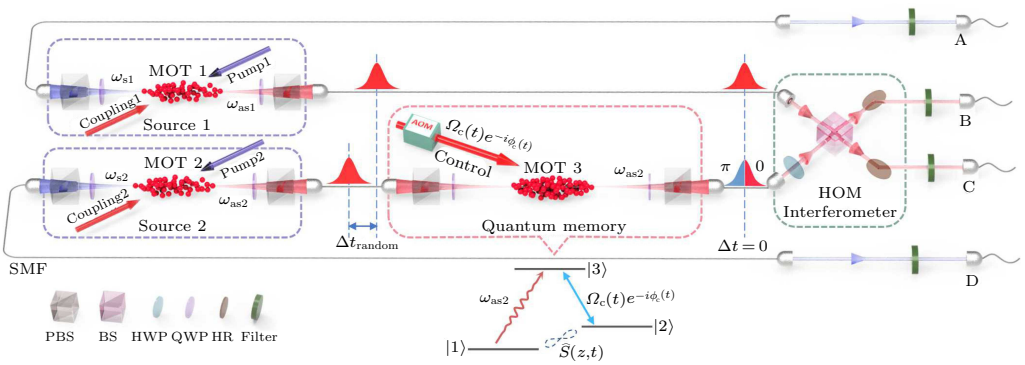

Fig. 1. Experimental setup. Three cigar-shape dense cold atomic ensembles are prepared by dark-line magneto-optical traps (MOT) of ^{85}Rb atoms. Single photons ω_{as1} (ω_{as2}) heralded by its counterpart ω_{s1} (ω_{s2}) are generated from MOT_1 (MOT_2) with the existence of pump1-coupling1 (pump2-coupling2) laser beams via the spontaneous four-wave-mixing process. Therefore, the timing differences between ω_{as1} and ω_{as2} are random and denoted by Δt_{random}. MOT_3 acts as an efficient QM based on EIT that can synchronize the readout single photon ω_{as2} to ω_{as1} ($\Delta t = 0$). As shown by the energy level schematics of EIT two-photon process, a control laser manipulates the storage and readout of single photons ω_{as2}. The amplitude and phase of the control laser pulse with a complex envelope of Rabi frequency $\Omega_c(t)e^{-i\phi_c(t)}$ is controlled by an acousto-optic modulator (AOM), by which the readout single photons ω_{as2} can be phase modulated accordingly. Single photons ω_{as1} and ω_{as2} are delivered to an HOM interferometer consisting of a beam splitter (BS) via single mode fibers (SMFs). Photons ω_{s1} and ω_{s2} are also collected and sent to detectors via SMFs. The generated photons are eventually detected by single photon counting modules (SPCMs) A, B, C and D. Filters are inserted before SPCMs to filter out noisy photons. PBS: polarization beam splitter, HWP: half wave plate, QWP: quarter wave plate, and HR: high reflection mirror.

The experimental setup shown in Fig. 1 contains three magneto-optical traps (MOT_1, MOT_2 and MOT_3) of ^{85}Rb atoms and an HOM interferometer. Cold atomic ensembles in MOT_1 and MOT_2 serve as two independent single photon sources. The dense cold atomic ensemble in MOT_3 serves as an efficient QM. Heralded single photons ω_{as1} and ω_{as2} are spontaneously and independently generated from MOT_1 and MOT_2, respectively; ω_{as2} can be stored in the QM immediately after its generation which is triggered by detecting an ω_{s2} photon. When a photon ω_{s1} is detected at the instant t_{s1}, the stored single photon ω_{as2} can be readout with a controllable delay respective to t_{s1} and then enter the HOM interferometer together with the single photon ω_{as1} that is also heralded by ω_{s1}.

Two single photon sources with exactly the same configuration are built based on MOT_1 and MOT_2 of ^{85}Rb atoms. We take MOT_1 as an example to illustrate the configuration. Laser cooled atoms are opti-

cally pumped to the lowest hyperfine level $|5S_{1/2}, F = 2\rangle$ before experimental window. Optical depth of atomic cloud is 120 on the transition $|5S_{1/2}, F = 2\rangle \rightarrow |5P_{1/2}, F = 3\rangle$, measured with a circularly polarized probe field. A pair of counter-propagating pumping laser beams pump$_1$ (780 nm, σ^-) and coupling laser beams coupling$_1$ (795 nm, σ^+) are shone on MOT$_1$ with an angle of 2.75° to the quantization axis. Counter-propagating entangled photon pairs are generated along the quantization axis. One of the photons, Stokes photon ω_{s1} is detected by single-photon counting modules (SPCM, Excelitas, SPCM-AQRH-16), which heralds the generation of an anti-Stokes photon ω_{as1}. The pump laser is blue detuned from the transition $|5S_{1/2}, F = 2\rangle \leftrightarrow |5P_{3/2}, F = 3\rangle$ by 150 MHz and focused on the center with a 0.82 mm $1/e^2$ diameter and power of 14 μW. The coupling laser, resonant to the transition $|5S_{1/2}, F = 3\rangle \leftrightarrow |5P_{1/2}, F = 3\rangle$, is collimated Gaussian beam with $1/e^2$ diameter of 1.8 mm and power of 3 mW. The optimal Gaussian-like single-photon temporal waveform is obtained following the optimization procedure described in Ref. [34]. Configuration of pump2 and coupling2 has slight difference in power and beam side. Laser pump2 has focal point spot diameter of 0.95 mm and power of 12.5 μW. Laser coupling2 is collimated with diameter of 1.8 mm and power of 4.5 mW. After detected by SPCMs, coincidence counts between photons are recorded by a time-to-digital converter (Fast Comtec P7888) with a time bandwidth of 2 ns. The experiment runs repeatedly with a rate of 50 Hz including an experimental window of 300 μs.

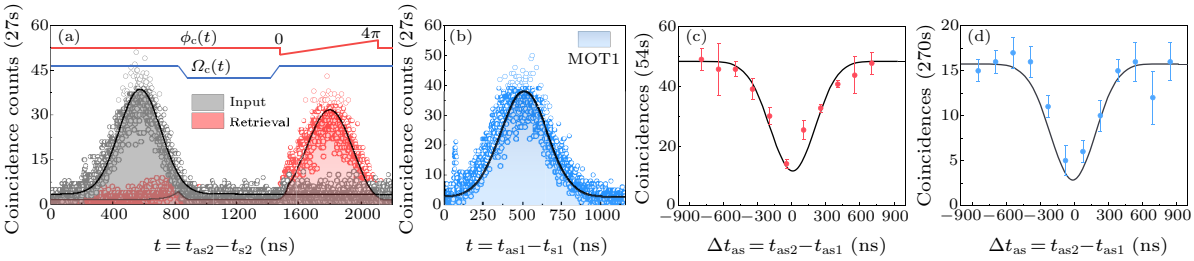

Fig. 2. Synchronized HOM interference. (a) Temporal waveforms of the single photons ω_{as2} (grey circles) and the readout single photons (red circles). The blue solid line denotes the results of switching off the control laser with a storage time of 700 ns. The red solid line depicts the linear phase modulation of the control laser from 0 to 4π. (b) The temporal waveform of the single photons ω_{as1} emitted from MOT$_1$ depicted with blue circles. The solid lines enclosing shadow areas are Gaussian fitted guide lines of the above temporal waveforms; τ is the detection time difference between paired $\omega_{s1,2}$ and $\omega_{as1,2}$. (c) and (d) Synchronized and conventional HOM interference pattern measured by fourfold coincidence counts of ω_{s1}, ω_{as1}, ω_{s2} and ω_{as2}. Red dots and blue dots are experimental data points with error bars. Black solid lines are theoretical curves.

In the experiments, single photons ω_{as1} and ω_{as2} are made almost indistinguishable by carefully tuning their polarization states, spatial modes, temporal and spectral profiles. Single photons ω_{as1} and ω_{as2} are experimentally generated in the same spontaneous four-wave-mixing processes that ensures they have the same polarization states and temporal and spectral profiles, where the optical depth (OD), the intensity and polarization of pump-coupling lasers and the focal point position of the pump laser are all carefully tuned in the photon sources of MOT$_1$ and MOT$_2$.[34] Their spatial modes before entering HOM interferometer are shaped the same by firstly being coupled into and then released out of the same type of singe mode fibers (SMFs). As shown in Figs. 2(a) and 2(b), the Gaussian shape temporal waveform likeness between ω_{as1} and ω_{as2} is 98.2% with a full width of half maximum of 320 ns. Meanwhile, the quantum nature of generated single photons are characterized by measuring their conditional auto-correlation function $g_c^{(2)}$ using the standard Hanbury Brown–Twiss interferometer. We have $g_c^{(2)}$ of 0.34 for both ω_{as1} and ω_{as2} photons, which verify their single photon quality.

To efficiently eliminate the arriving time difference at the HOM interferometer, a QM built in MOT$_3$ that is optimized for single photon ω_{as2} is inserted between MOT$_2$ and the HOM interferometer. The QM is made in cold atomic ensemble of ^{85}Rb atoms prepared in MOT$_3$.[22] Atoms are pumped to Zeeman sublevel $|1\rangle = |5S_{1/2}, F = 2, m_F = 2\rangle$ before experimental window. Atomic OD 400 is measured on the transition $|1\rangle \leftrightarrow |3\rangle = |5P_{1/2}, F = 3, m_F = 3\rangle$ for circularly polarized anti-Stokes field. The control laser is tuned to be resonant transition between $|3\rangle \leftrightarrow |2\rangle = |5S_{1/2}, F = 3, m_F = 2\rangle$. The single photon field is focused at the center of MOT$_3$ with a beam waist radius of 150 μm. The control laser shines on atomic cloud with an angle of 1° and a $1/e^2$ diameter 4.7 mm. As shown in Fig. 2(a), a high storage efficiency of 86% is achieved in our QM. Additionally, the temporal waveform likeness (98.5%) of photon ω_{as2} together with its polarization state, spatial modes, frequency and single-photon nature [$g_c^{(2)} = 0.43$] are all well-preserved during the storage-readout process.

HOM interferences with and without QM are experimentally compared in our work. In Fig. 2(c), the

QM assisted HOM interference shows an HOM visibility of 76%. The horizontal axis denotes the arrival time delay $\Delta t_{\rm as}$ between single photons $\omega_{\rm as1}$ and $\omega_{\rm as2}$, which is swept by controlling the storage time of $\omega_{\rm as2}$ with a step of 150 ns. The coincidence counts are measured at the exit ports of the HOM interferometer with an integration window of 640 ns that covers the whole single-photon wavepacket. The results from conventional HOM interference are plotted in Fig. 2(d), where single photons $\omega_{\rm as1}$ and $\omega_{\rm as2}$ enter the HOM interferometer randomly. The HOM interference pattern is obtained by passively analyzing the fourfold coincidence events with respect to their arrival time difference $\Delta t_{\rm as} = t_{\rm as2} - t_{\rm as1}$ for QM assisted HOM and $\Delta t_{\rm as} = t_{\rm s2} - t_{\rm s1}$ for HOM without a QM. The visibility of HOM dip measured in this way is 82%, which is mainly limited to the finite distinguishability of photons from the source. Using the experimental data shown in Figs. 2(c) and 2(d), the measured coincidence rates are $0.89\,{\rm s}^{-1}$ and $0.06\,{\rm s}^{-1}$, respectively. Therefore, the detected four-photon coincidence rate of synchronized the HOM interference is improved by a factor of around 15 compared to that of the conventional HOM interference. The coincidence rate is limited by the finite storage time of 5 μs in our work and can be further improved if the storage time is longer.

The fourfold coincidence is acquired by analyzing the counting relation of $\omega_{\rm s1}$, $\omega_{\rm s2}$, $\omega_{\rm as1}$ and $\omega_{\rm as2}$ photons. After HOM interferometer, the fourfold coincidence rate reads[13]

$$\begin{aligned} P^{(4)} =& T^2 \int d\tau |\psi_1(\tau)|^2 + R^2 \int d\tau |\psi_2(\tau)|^2 \\ & - 2TR| \int d\tau \psi_1^*(\tau)\psi_2(\tau+\Delta t)|^2 \\ & + TR\tilde{g}^{(2)} \int d\tau |\psi_1(\tau)|^2 \int d\tau |\psi_2(\tau)|^2, \quad (3) \end{aligned}$$

where $\psi_1(\tau)$ $[\psi_2(\tau)]$ is the single photon wave packet function of $\rm MOT_1$ ($\rm MOT_2$), and τ is relative delay between $\omega_{\rm as1}$ and $\omega_{\rm as2}$. The Δt is time difference of $\omega_{\rm s1}$ and $\omega_{\rm s2}$. T and R refer to the transmission and reflection of BS, respectively. The $\tilde{g}^{(2)}$ is the average value of $g^{(2)}$ within whole wave packet.

From Eq. (1), by modulating the phase of control laser $\phi_{\rm r}(t - t_{\rm r})$ during the readout process, the readout single photon might be phase modulated in the same way. Although the amplitude envelope of the readout single photons can also be modulated in the same way, in our current work, the amplitude of control laser envelopes is optimized for keeping a high storage efficiency.[22] We firstly realize a step phase change of π of the readout single photon and verify it in our HOM interferometer. In principle, the different phase envelopes make two input photons completely distinguishable and would destroy the HOM dip when the whole single photon wavepackets are take into account, which means that all the interference events are simply counted. However, when observing the HOM interference of the partial wavepacket of two single photons, we may still obtain interesting HOM interference pattern.[11] We thus investigate the HOM interference pattern in the time domain by separating the photon wavepacket into two halves ($|e\rangle$ is the earlier half, and $|l\rangle$ is the later half).

When dynamical varying the phase of one photon, the photon coincidence between two BS output port becomes phase-dependent. The coincidence rate is[11]

$$P^2 = |\psi_1(\tau)|^2 |\psi_1(\tau)|^2 \sin(\pi \Delta\nu\tau), \quad (4)$$

where $\Delta\nu$ is phase-varying-induced frequency difference. In our linear phase shaping result, for 4π variation within 540 ns, the phase-varying-induced frequency difference is 3.7 MHz.

When photon coincidence is detected in the same halves $|e,e\rangle$ or $|l,l\rangle$, as illustrated in Fig. 3(a), the photons behave in a coalescence way and tend to exit at the same out port of BS as expected, because the two input states $|e,e\rangle$ and $|l,l\rangle$ are temporally separated and thus each input paired half can be viewed as regular HOM interference. The interfered two-photon wavepacket is shown in Fig. 3(b), where the coincidence count is significantly reduced to only 30% of that of the non-interference case. The non-interference coincidence count is measured by intentionally adjusting the polarization states of single photons $\omega_{\rm as1}$ and $\omega_{\rm as2}$ to be orthogonal to each other and thus making them distinguishable. However, when photon coincidence is detected in different halves of the wavepacket $|e,l\rangle$ (or $|l,e\rangle$), as illustrated in Fig. 3(c), photons behave in an anti-coalescence way. Take the detected output state $|e,l\rangle$ as an example, the reflected input state of $|e,-l\rangle \to |e,l\rangle$ and the transmitted input state $|e,l\rangle \to |e,l\rangle$ constructively interfere at the exit ports of BS. When the phase of the read-out single photon is modulated, the interfered two-photon wavepacket shown in Fig. 3(d) reveals that the coincidence count increases up to 170% compared to the non-interference case. Our results verify that a step phase modulation of π of the readout single photon $\omega_{\rm as2}$ via QM is realized, which agrees well with the theoretical prediction of coincidence count changes of 0% and 200%.

In addition, we demonstrate a linear phase modulation of 4π spanned over the whole single photon wavepacket. As shown in Fig. 3(f), with a linear phase modulation within 540 ns, the expected oscillation structure in the interfered two-photon wavepacket can be clearly observed. The experimental data points (blue dots) agree well with the theoretical curves (black solid line) with an oscillation period of 270 ns, which is the time for generating 2π phase modula-

tion. Alternatively, this oscillation structure is the beating signal in two-photon interference when two input photons have a finite center frequency difference introduced by linear phase modulation.[35] Therefore, the above results clearly show that arbitrary phase modulation can be realized together with the storage-readout processes of an EIT-based QM while the storage efficiencies are kept above 86%.

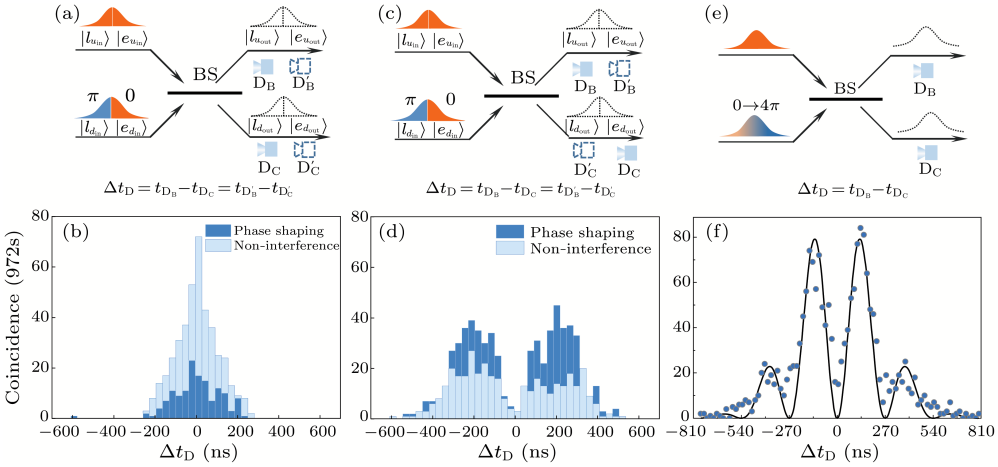

Fig. 3. Step and linear phase modulation of readout single photon. [(a), (c), (e)] Schematics of detecting the two-photon wavepacket out of the HOM interferometer. Δt_D is the detection time delay. In (a) and (b), the two photons are detected in either the early ($|e,e\rangle$ at t_{D_B} and t_{D_C}) or latter ($|l,l\rangle$ at $t_{D_B'}$ and $t_{D_C'}$) half of the wavepacket. In (c) and (d), the two photons are detected in different halves of the wavepackets by ($|l,e\rangle$ at t_{D_B} and t_{D_C}) or ($|e,l\rangle$ at $t_{D_B'}$ and $t_{D_C'}$). [(b), (d)] Two photon coincidences with time bin width of 32 ns. The dark and light blue histograms show the interfered and non-interfered coincidence results, respectively. Owing to the finite rise time of the phase modulator, photons detected within ± 25 ns are omitted from the above data. In (e), Δt_D is the detection time delay when a photon is detected by D_B at time t_{D_B} and another photon is detected by D_c at time t_{D_c}. (f) Two photon coincidences with time binwidth of 18 ns. The blue dots show the experimental data points. The black solid line is the theoretical curve.

In conclusion, we have developed a phase modulator built in an EIT-based atomic QM. Synchronized HOM interference of spontaneously generated single photons is demonstrated with the assistance of a QM. The interference rate increases by a factor of 15 compared to the conventional case based on post-selection. Furthermore, the phase modulation of the readout single photon wavepacket out of QM is demonstrated while quantum storage performance remains high. Both step phase modulation and linear phase modulation of the read-out single photon are realized by directly modulating the phase envelope of the control laser. The coalescence and anti-coalescence behaviors in the HOM interference are explored by observing the two-photon wavepacket out of the interferometer, which successfully verifies the expected phase modulation of single photons.

Our single photon phase modulator causes no additional photon loss and thus would be of broad interest to multiple research areas in quantum information processing, such as memory required quantum communication,[6,7,18,36] quantum information processing using temporal modes of single photons,[10] and quantum computation using linear optics.[37]

We thank both Professor Peng Xu from Wuhan Institute of Physics and Mathematics of the Chinese Academy of Sciences and Professor Jiefei Chen from Southern University of Science and Technology for their useful discussions.

References

[1] Hong C K, Ou Z Y and Mandel L 1987 *Phys. Rev. Lett.* **59** 2044
[2] Kok P, Munro W J, Nemoto K, Ralph T C, Dowling J P and Milburn G J 2007 *Rev. Mod. Phys.* **79** 135
[3] Duan L M, Lukin M D, Cirac J I and Zoller P 2001 *Nature* **414** 413
[4] Sangouard N, Simon C, de Riedmatten H and Gisin N 2011 *Rev. Mod. Phys.* **83** 33
[5] Kimble H J 2008 *Nature* **453** 1023
[6] Wehner S, Elkouss D and Hanson R 2018 *Science* **362** eaam9288
[7] Bhaskar M K, Riedinger R, Machielse B, Levonian D S, Nguyen C T, Knall E N, Park H, Englund D, Lončar M, Sukachev D D and Lukin M D 2020 *Nature* **580** 60
[8] Inoue K, Waks E and Yamamoto Y 2002 *Phys. Rev. Lett.* **89** 037902
[9] Marcikic I, de Riedmatten H, Tittel W, Zbinden H, Legré M and Gisin N 2004 *Phys. Rev. Lett.* **93** 180502
[10] Raymer M G and Walmsley I A 2020 *Phys. Scr.* **95** 064002
[11] Specht H P, Bochmann J, Mücke M, Weber B, Figueroa E, Moehring D L and Rempe G 2009 *Nat. Photon.* **3** 469
[12] Pan J W, Chen Z B, Lu C Y, Weinfurter H, Zeilinger A and Żukowski M 2012 *Rev. Mod. Phys.* **84** 777
[13] Qian P, Gu Z, Cao R, Wen R, Ou Z Y, Chen J F and Zhang W 2016 *Phys. Rev. Lett.* **117** 013602
[14] Liu S, Lai X, Yang C and Chen J F 2021 *Chin. Phys. Lett.* **38** 084201
[15] Bussières F, Sangouard N, Afzelius M, de Riedmatten H, Simon C and Tittel W 2013 *J. Mod. Opt.* **60** 1519

[16] Nunn J, Langford N K, Kolthammer W S, Champion T F M, Sprague M R, Michelberger P S, Jin X M, England D G and Walmsley I A 2013 *Phys. Rev. Lett.* **110** 133601
[17] Kaneda F, Xu F, Chapman J and Kwiat P G 2017 *Optica* **4** 1034
[18] Jing B, Wang X J, Yu Y, Sun P F, Jiang Y, Yang S J, Jiang W H, Luo X Y, Zhang J, Jiang X, Bao X H and Pan J W 2019 *Nat. Photon.* **13** 210
[19] Boller K J, Imamoğlu A and Harris S E 1991 *Phys. Rev. Lett.* **66** 2593
[20] Hsiao Y F, Tsai P J, Chen H S, Lin S X, Hung C C, Lee C H, Chen Y H, Chen Y F, Yu I A and Chen Y C 2018 *Phys. Rev. Lett.* **120** 183602
[21] Vernaz-Gris P, Huang K, Cao M, Sheremet A S and Laurat J 2018 *Nat. Commun.* **9** 363
[22] Wang Y, Li J, Zhang S, Su K, Zhou Y, Liao K, Du S, Yan H and Zhu S L 2019 *Nat. Photon.* **13** 346
[23] Reim K F, Nunn J, Lorenz V O, Sussman B J, Lee K C, Langford N K, Jaksch D and Walmsley I A 2010 *Nat. Photon.* **4** 218
[24] Ding D S, Zhang W, Zhou Z Y, Shi S, Shi B S and Guo G C 2015 *Nat. Photon.* **9** 332
[25] Guo J, Feng X, Yang P, Yu Z, Chen L Q, Yuan C H and Zhang W 2019 *Nat. Commun.* **10** 148
[26] Fleischhauer M and Lukin M D 2000 *Phys. Rev. Lett.* **84** 5094
[27] Patnaik A K, Kien F L and Hakuta K 2004 *Phys. Rev. A* **69** 035803
[28] Chen B, Qiu C, Chen S, Guo J, Chen L Q, Ou Z Y and Zhang W 2015 *Phys. Rev. Lett.* **115** 043602
[29] Qiu C, Chen S, Chen L Q, Chen B, Guo J, Ou Z Y and Zhang W 2016 *Optica* **3** 775
[30] Guo X, Mei Y and Du S 2018 *Phys. Rev. A* **97** 063805
[31] Mair A, Hager J, Phillips D F, Walsworth R L and Lukin M D 2002 *Phys. Rev. A* **65** 031802
[32] Lukin M D 2003 *Rev. Mod. Phys.* **75** 457
[33] Jeong T, Park J and Moon H S 2017 *Sci. Rep.* **7** 15559
[34] Li J F, Wang Y F, Su K Y, Liao K Y, Zhang S C, Yan H and Zhu S L 2019 *Chin. Phys. Lett.* **36** 074202
[35] Legero T, Wilk T, Hennrich M, Rempe G and Kuhn A 2004 *Phys. Rev. Lett.* **93** 070503
[36] Yan H, Zhu S L and Du S W 2011 *Chin. Phys. Lett.* **28** 070307
[37] Knill E, Laflamme R and Milburn G J 2001 *Nature* **409** 46